

# Longitudinal characterization of the Wallerian degeneration process by a multi-compartment diffusion model: DIAMOND after a rhizotomy in the rat spinal cord and comparison with the histology

Damien Jacobs<sup>1</sup>, Benoit Scherrer<sup>2</sup>, Aleksandar Jankovski<sup>3</sup>, Anne des Rieux<sup>4</sup>, Maxime Taquet<sup>1</sup>, Bernard Gallez<sup>4</sup>, Simon K. Warfield<sup>2</sup>, and Benoit Macq<sup>1</sup>

<sup>1</sup>ICTEAM, Université catholique de Louvain, Louvain-La-Neuve, Belgium, <sup>2</sup>Computational Radiology Laboratory, Boston Childrens Hospital, Massachusetts, United States, <sup>3</sup>Hopital universitaire Mont-Godinne, Université catholique de Louvain, Godinne, Belgium, <sup>4</sup>LDRI, Université catholique de Louvain, Brussels, Belgium

**Purpose:** To investigate the Wallerian degeneration process by DIAMOND<sup>1</sup>, a multi-compartment diffusion model, in the rat spinal cord after a rhizotomy. With a longitudinal imaging approach and several histological observations for each specific cellular response, the fluctuations of the diffusion parameters are analyzed and compared to the Wallerian degeneration process in the course of time.

**Methods:** A left-unilateral rhizotomy was performed on 6 rats at L2-L3 levels inducing Wallerian degeneration in the ipsilateral gracile fasciculus. A laminectomy was also performed on 3 control rats at identical L2-L3 levels (shams). For each rat, diffusion weighted imaging (DWI) was performed at 11.7T, in vivo, before the surgery (pre-surgery), after 4, 13, 37 and 51 days post-injured with 12 non-weighted DW images and 6 shells of 36 gradients directions each at b-values: 300, 700, 1500, 2800, 4500, 6000 s/mm<sup>2</sup>, non collinear directions<sup>2</sup>, voxel resolution: 0.1x0.1x1 mm<sup>3</sup>, TE: 23ms,  $\delta$ : 4.5ms,  $\Delta$ : 12 ms. After the acquisition at 51 or 37 post-surgery days (3 rats for each group.), rats were perfused, spinal cord was removed, cryoprotected before being frozen and stored at -80°C, sliced axially in 20  $\mu$ m thick section using cryostat. Four immunostainings and one stain were performed for the myelin (LFB), neurofilaments (SMI312), oligodendrocytes (ab7474), microglia (Iba1), and astrocytes (GFAP). For each imaging dataset, DW images were resampled to 0.1x0.1x0.1mm<sup>3</sup> and corrected for animal motion and eddy-current distortion using affine registration to the b=0 s/mm<sup>2</sup> image. DIAMOND's model parameters were estimated using the CRL Toolkit, considering one isotropic compartment and one anisotropic compartment. DIAMOND estimates a continuous distribution of diffusion tensors. The expectation of the 6-D distribution of diffusion tensors provides the overall diffusivity of each compartment, and its concentration provides a measure of the overall compartment heterogeneity (heterogeneity index, *hei*). The diffusivity parameters ( $\lambda_{\parallel}$ ,  $\lambda_{\perp}$ ) of a fascicle and the isotropic diffusivity ( $D_{iso}$ ) are estimated from the data. For each imaging time point, we tested whether average parameter values in the ipsilateral of the spinal cord were significantly different ( $\alpha=0.05$ ) after rhizotomy and compared to the pre-surgery (including shams). Due to the non-normality of the data's (normality test evaluation), the Kruskal-Wallis test was performed and combined with a multi comparison post-hoc test (Tukey-Kramer) to determine the statistical significance between the groups of different time points.

**Results** (presented for 3 rats): For the shams, the neurofilament structure is preserved on the Fig1 a.1 and the fibrous structure of the myelin is also observed on the Fig1 b.1. After 51 days post-surgery, the axonal degeneration is characterized by the absence of neurofilaments on the Fig1 a.2. For the LFB staining, the density of myelin is lower for the rhizotomy group than the shams and a morphological "dot" structure is observed on the Fig1 b.2. For the astrocytes, a cellular activation is observed in the injured tissue on the Fig1 c.2 in comparison with the shams (Fig1 c.1). For the microglia staining, a vesicular activation is illustrated on the Fig1 d.2 for the injured group. For the sham, the density of microglia per unit of area is lower than the injured group in the gray matter and the white matter. For the oligodendrocyte, the fibrous structure is observed for the shams (Fig1 e.1). After the rhizotomy, the cellular morphology is less structured and the diameter of the body cell is larger. For DIAMOND, after 4 days, the axial diffusivity,  $\lambda_{\parallel}$ , drops off to 1.6  $\mu$ m<sup>2</sup>/ms but the radial diffusivity,  $\lambda_{\perp}$ , remains close to 0.2  $\mu$ m<sup>2</sup>/ms. The isotropic diffusion coefficient,  $D_{iso}$ , decreases from 3 to 1.9  $\mu$ m<sup>2</sup>/ms and its fraction  $f_{D_{iso}}$  increases from 0.14 to 0.24 significantly. A significant increase of the heterogeneity index, *hei*, is also observed between the pre-surgery and 4 post-surgery days. At 13 post-surgery days,  $\lambda_{\parallel}$  increase from 1.6 to 1.75  $\mu$ m<sup>2</sup>/ms significantly and the radial diffusivity increases slightly and significantly. The mean of  $D_{iso}$ ,  $f_{D_{iso}}$  and *hei* do not change significantly between the 4 and 13 post-surgery days. After 37 post-surgery days,  $\lambda_{\parallel}$  increases significantly and is returned to a value close to the free diffusivity, at 2.7  $\mu$ m<sup>2</sup>/ms. The  $D_{iso}$  drops off to 1  $\mu$ m<sup>2</sup>/ms and its fraction increases to 0.35, significantly. At 51 days post-surgery,  $\lambda_{\parallel}$  remains close to 2.7  $\mu$ m<sup>2</sup>/ms but  $\lambda_{\perp}$  increases significantly from 0.2 to 0.3  $\mu$ m<sup>2</sup>/ms. The  $D_{iso}$  and its fraction do not change from the 37 post-surgery days and remain close to 1  $\mu$ m<sup>2</sup>/ms and 0.35 respectively.

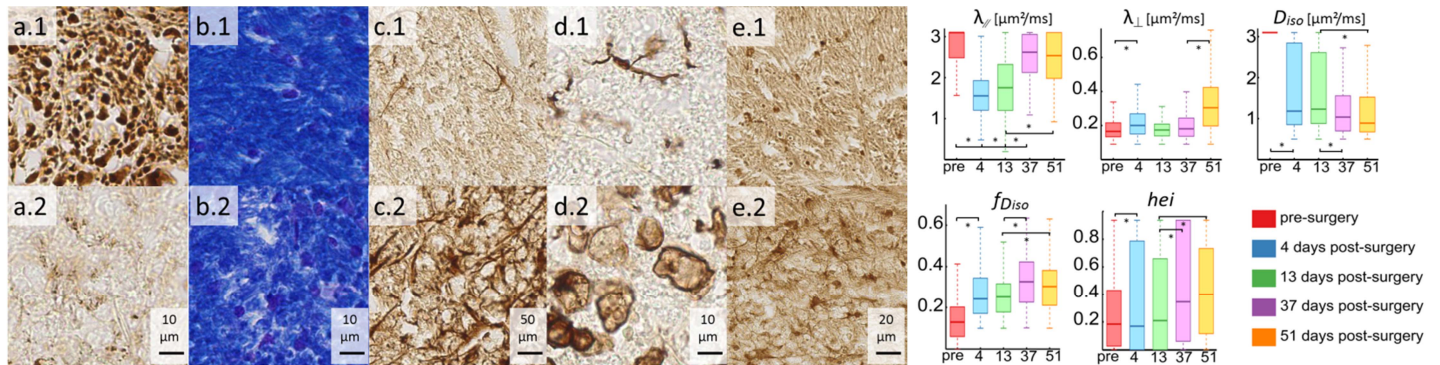


Figure 1 : 1 vs 2 : sham vs rhizotomy, (a.1-a.2) Neurofilament (SMI-312), (b.1-b.2), Myelin (LFB), (c.1-c.2) Astrocyte (GFAP), (d.1-d.2) Microglia (Iba-1), (e.1-e.2) Oligodendrocyte (ab7474). DIAMOND parameters at pre surgery, 4, 13, 37, 51 post-surgery days for axial  $\lambda_{\parallel}$ , radial  $\lambda_{\perp}$ , isotropic  $D_{iso}$ , diffusivities, fraction of  $D_{iso}$   $f_{D_{iso}}$ , and heterogeneity index, *hei*.

**Discussion:** In the Wallerian degeneration process, the acute axonal degeneration occurs in the first days after the rhizotomy with the axolemma degradation and the granular disintegration of the axonal cytoskeleton<sup>3</sup>. In this first step, the myelin structure is not altered and the presence of axonal debris could explain the significant decrease of the  $\lambda_{\parallel}$  parameter after 4 days. The increase of *hei* could also be sensitive to this first axonal degeneration period. After 13 days, most of diffusion parameters remain constant and at 37 days,  $\lambda_{\parallel}$  returns to 2.7  $\mu$ m<sup>2</sup>/ms. The return close to the free diffusion value could be set against the total degradation and clearance of axons. The neurofilament staining at 37 days post-surgery tends to support this hypothesis. The myelin clearance is a second major step that occurs in the CNS and over several months. At 37 days, the significant decrease of the  $D_{iso}$  could be related to the vesicular and astrocyte activations required for the myelin clearance<sup>4</sup>. The significant increase of  $\lambda_{\perp}$  at 51 days coupled to a low  $D_{iso}$  could be an indicator for the myelin clearance.

**Conclusion:** The evolution of the DIAMOND parameters regarding the histological observations suggests that this model could be sensitive to the different cellular responses during the Wallerian degeneration process.

[1]. Scherrer, B., et al., Characterizing the Distribution of Anisotropic Micro-structural Environments with Diffusion-weighted imaging (DIAMOND). Med Image Comput Assist Interv., 2013. 16: p. 518-526. [2] Caruyer, E., et al., Design of multishell sampling schemes with uniform coverage in diffusion MRI. Magn Reson Med, 2013. 69(6): p. 1534-40. [3] Vargas, Mauricio E.; Barres, Ben A. "Why Is Wallerian Degeneration in the CNS So Slow?". Annual Review of Neuroscience 30 (1): 153-179. [4] Skripuletz T et al., Astrocytes regulate myelin clearance through recruitment of microglia during cuprizone-induced demyelination., Brain, 2013 136: p. 147-167